Photoionization of atomic scandium in the ground state: Total cross sections and $3p \rightarrow 3d$ resonances

Zikri Altun*
Department of Physics, Marmara University, Istanbul, Turkey

Steven T. Manson†
Department of Physics and Astronomy, Georgia State University, Atlanta, Georgia 30303

(Received 5 November 1998)

A methodology is developed combining many-body-perturbation theory and close coupling of final-state channels with multiconfiguration Hartree-Fock theory to calculate photoionization cross sections of open-shell atoms with accurate threshold and resonance energies. Photoionization calculations of the ground $1s^2 2s^2 2p^6 3s^2 3p^6 3d 4s^2\ D$ state of atomic Sc, the first of the transition metals, are performed from threshold to 60 eV using this method. All single-electron transitions from $4s$, $3d$, and $3d$ subshells are included. Over a broad region of energy, the cross section is dominated by the strength of the $3p \rightarrow 3d$ resonances which are split into nine distinct transitions through the angular momentum coupling with the open shells. The total cross section and the $3p \rightarrow 3d$ resonances are presented in detail and reasonably good agreement with available experiment, for both energies and cross section, is obtained. Classifications of a number of the $3p \rightarrow 3d$ resonances are proposed. In the low-energy region, good agreement with a previous *R*-matrix calculation is found. [S1050-2947(99)07505-8]

PACS number(s): 32.80.Fb, 32.80.Hd, 32.80.Dz

I. INTRODUCTION

Photoionization of atoms is one of the basic processes of nature. It is also crucial in many applications [1], e.g., astrophysics and radiation physics. In addition, atomic results often carry over in whole or in part to molecular and condensed-matter systems [2], since atoms are the elementary particles of molecules and solids.

In recent years, atomic photoionization studies have been spurred on by the advent of third-generation synchrotron radiation sources [3], which make it possible to explore processes that were inaccessible just a few years ago. In a parallel development, the upsurge in the availability of computational power has provided significantly enhanced calculational capabilities. At this point, there is significant amounts of data, both experimental and theoretical, on the noble gases and, to a lesser extent, on other closed subshell atoms [4]. But most of the periodic table consists of open-shell atoms. There is some data on the alkali-metal atoms and some other atoms with unfilled *p* subshells, and understanding of these atoms is developing. But the photoionization of atoms with open *d* and *f* subshells is largely unexplored [4,5].

As a first step toward developing a greater understanding of such systems, the photoionization cross section of Sc in the ground state has been investigated. This choice was dictated by the fact that Sc, with a ground-state structure $1s^2 2s^2 2p^6 3s^2 3p^6 3d 4s^2\ ^2D$, is the lowest member of the periodic system to include a *d* electron in the ground state. This study represents part of a broader effort to understand the details of the photoionization of the $3d$ transition-metal atoms and ions, particularly in the region of the $3p \rightarrow 3d$ resonance transitions. This region is of great interest because these $3p \rightarrow 3d$ transitions are extremely strong, owing to the fact that they are $\Delta n = 0$ transitions, and they dominate the cross section wherever they occur. In addition, experiment has shown that the nature of these resonances changes dramatically [5] from Sc to Ni, evolving from widely distributed in Sc to highly concentrated in Ni. To understand this behavior, of course, requires a detailed study of each of the elements.

The cross sections reported herein include photoionization of $4s$, $3d$, and $3p$ electrons of the ground state of Sc. Excluding ionization plus excitation, which is not considered here, all possible photoionizing transitions involving these electrons leads to nine final ionic states and 32 channels as follows ($[\mathrm{Mg}] = 1s^2 2s^2 2p^6 3s^2$):

$$([\mathrm{Mg}] 3p^6 3d 4s\ ^{1,3}D) kp\ ^2P,D,F, \tag{1}$$

$$([\mathrm{Mg}] 3p^6 4s^2\ ^1S) kp\ ^2P,\ \ kf\ ^2F, \tag{2}$$

$$([\mathrm{Mg}] 3p^5 3d 4s^2\ ^{1,3}F) ks\ ^2F,\ \ kd\ ^2P,D,F, \tag{3}$$

$$([\mathrm{Mg}] 3p^5 3d 4s^2\ ^{1,3}D) ks\ ^2D,\ \ kd\ ^2P,D,F, \tag{4}$$

$$([\mathrm{Mg}] 3p^5 3d 4s^2\ ^{1,3}P) ks\ ^2P,\ \ kd\ ^2P,D,F, \tag{5}$$

with $k = n$ for discrete (autoionizing) transitions and $k = \varepsilon$ for ionization. The calculation is performed in *LS* coupling and correlation is included using a combination of many-body-perturbation theory (MBPT) for the weaker perturbations, such as those affecting the ground state, and a matrix diagonalization technique plus perturbation theory to treat the strong interactions among the final degenerate open and closed channels. The calculation covers the energy range from the first ionization threshold to a photon energy of 60

*Electronic address: zikalt@superonline.com
†Electronic address: smanson@gsu.edu

eV, just below the resonances leading up to the $3s$ thresholds; $3s$ excitation/ionization was not considered in this work.

This study may be considered as a complement to an earlier theoretical work [6,7] which treated the energy region from the first ionization threshold to about 1 eV above to very high accuracy, including ionization plus excitation and spin-orbit splittings. In this narrow energy region, comparison of the results obtained by vastly dissimilar theoretical techniques provides an excellent indication of accuracy. But the present study really concentrates on the higher-energy region where detailed accurate calculations are scarce and experiment is fragmentary [5] in an effort to detail the oscillator strength distribution in this region. In this first paper the theoretical methodology is presented, along with the total cross section, the $3p \rightarrow 3d$ resonances, and comparison with available experiment. In a subsequent paper, the subshell and channel cross sections, along with the Rydberg resonance positions and decay channels, will be discussed.

II. THEORY AND CALCULATION

A detailed description of a part of the theoretical methodology was presented earlier [8], so only a brief description of that part is given here. Within the framework of the electric dipole approximation, which is excellent for low-energy photoabsorption processes, the cross section for a transition from initial state i to final state f via absorption of a photon of energy $\hbar\omega$, is given by [9]

$$\sigma_{\mathrm{if}} = \frac{4\pi^2\omega}{g_i c} \left| \vec{\epsilon} \cdot \left\langle \psi_i \left| \sum \vec{r}_j \right| \psi_f \right\rangle \right|^2, \tag{6}$$

where g_i is the multiplicity of the initial state, c is the speed of light, and $\boldsymbol{\epsilon}$ is the photon polarization. In Eq. (6), summing over final, and averaging over initial, magnetic substrates is implied. Equation (6) is given in the so-called length formulation; alternate forms of the dipole matrix element [10], known as velocity or acceleration forms, which yield identical results for exact wave functions, exist, and these are useful as indicators of the accuracy of the results [9].

The calculational methodology is an outgrowth of the MBPT techniques pioneered by Boyle, Altun, and Kelly [8].

A. Calculation of the dipole matrix element and correlations

The calculation is started by generating the Hartree-Fock (HF) orbitals for the $1s^2 2s^2 2p^6 3s^2 3p^6 3d 4s^2\ ^2D$ ground state of Sc, using the code of Froese Fischer [11]. Then, using an optimized single-particle Hamiltonian [8,12], the basis set is extended to excited orbitals for $l = 0-3$ up to $n = 13$ in the discrete energy range, and a grid of continuum orbitals with energies from 0 to 96 a.u. ($\approx$2600 eV). Using the discrete and continuum orbitals thus generated, the lowest-order wave functions for the various final states, as enumerated in Eqs. (1)–(5), are generated; the optimized single-particle Hamiltonian allows us to construct lowest-order final states which are both solutions to the same Hamiltonian as the initial state, and very close to the true HF for these final states. The lowest-order dipole matrix elements for transitions to the various final states are computed; these give essentially the unrelaxed HF cross sections.

Ground-state correlation is introduced by using first-order perturbation theory to correct the ground-state HF wave function, i.e., states involving one- and two-particle excitations from the HF ground state of Sc which also have a nonzero dipole matrix element with at least one of the final states [Eqs. (1)–(5)] are included. Sums are carried out explicitly over discrete states up to $n = 13$, and an extrapolation procedure is used to include the effects of the remaining discrete states [13]. The sum becomes an integral over continuum states and is performed explicitly. The lowest-order dipole matrix elements are then corrected for these ground-state correlations. We have investigated *all* first-order corrections which contribute to the various dipole matrix elements relevant to the calculation, and have included all those that have an appreciable effect; it turns out that only mixings with $3p^6 3d 4s k d$ and $3p^5 3d 4s^2 k f$ $(k = n, \varepsilon)$ are not included, because their effects are so small.

These corrections to the ground-state wave function, and thereby the dipole matrix elements, are relatively small, since the Coulomb matrix elements connecting the ground state to the other states are small compared to the energy differences. Thus perturbation theory should provide a good description of these corrections. To check this further, however, the second-order corrections which we believe to be the largest, terms involving $3p^5 3d 4s^2 k f$ intermediate states, are included in the calculation; their effect is negligible. This further supports the adequacy of using perturbation theory to include the effects of these initial-state correlations on the dipole matrix elements.

The final states present a different challenge, because they are often degenerate and can interact strongly. Thus, rather than use perturbation theory, the Hamiltonian matrix, defined by the subspace of final-state channels enumerated in Eqs. (1)–(5), is diagonalized, which leads to dipole matrix elements corrected for this final-state correlation. This is equivalent to infinite-order perturbation theory restricted to the subspace. However, prior to diagonalization, this matrix is modified, using perturbation theory, to include higher-order interactions among the final states involving intermediate states outside the subspace, i.e., we include the effects of channels omitted from the calculation on the channels that are explicitly included. Experience, plus a number of test calculations, has led us to the states arising from the $3p^4 3d^3 4s \varepsilon p$ configuration, which affect the strong $3p \rightarrow 3d$ transitions, as the most important intermediate states. Also investigated were $3p^5 3d^2 k p \varepsilon p$, $3p^5 3d 4s k f \varepsilon p$, and $3p^5 3d 4s k p \varepsilon f$ intermediate final states, summed to infinite order, but their effects proved to be small so they were neglected. Also included, however, was a higher-order simultaneous initial- and final-state correlation, also summed to infinite order, where the initial state is mixed with $3p^5 3d^2 4s \varepsilon p$ and the final state is mixed with $3p^4 3d^3 4s \varepsilon p$. Up to this point, the calculation is quite similar to the description given in Ref. [8].

B. Threshold energies

In order to obtain the best *ab initio* threshold energies, MBPT has not been used. The energies of the various thresholds were obtained by performing multi-configuration Hartree-Fock (MCHF) [14] calculations on the initial state of

TABLE I. Threshold energies, in eV, calculated using the MCHF approximation for the various channels included in the calculation compared with available experiment [15] and previous theory [16].

Sc^+ State	MCHF	Experiment	Previous theory
$3p^6 3d4s\ ^3D$	6.539	6.560	
$3p^6 3d4s\ ^1D$	6.772	6.875	
$3p^6 4s^2\ ^1S$	7.979	8.015	
$3p^5 3d4s^2\ ^3P$	37.96		37.8
$3p^5 3d4s^2\ ^3F$	39.31		39.1
$3p^5 3d4s^2\ ^1D$	41.31		40.9
$3p^5 3d4s^2\ ^1F$	41.81		41.8
$3p^5 3d4s^2\ ^3D$	42.16		40.9
$3p^5 3d4s^2\ ^1P$	51.26		

Sc, along with the various ionic states of Sc^+, and taking the difference. To obtain the energies of the various states of Sc^+, along with the ground state of Sc, we have used approximately 500 basis states in each MCHF calculation. The three lowest states of Sc^+ considered, $4s^{-1}\ ^3D$, $4s^{-1}\ ^1D$, and $3d^{-1}\ ^1S$, are each the lowest states of Sc^+ of their respective symmetries, as is the ^2D ground state of neutral Sc, so that the MCHF procedure yields a true upper bound for each of these states. On the other hand, the six $3p^{-1}$ odd-parity $^{1,3}P,D,F$ states are not the lowest of their respective symmetries; there are an infinite number of $3p^6 nln'l'$ odd-parity states of Sc^+ below the $3p^{-1}$ states. We have performed HF calculations on the lowest state of each symmetry, e.g., $3p^6 4s4p\ ^{1,3}P$. To insure orthogonality to these lower-energy odd-parity states of the same symmetry, and thereby insure upper bounds, in the MCHF calculation for the $3p^{-1}$ states of Sc^+, the orbitals appearing in the HF calculations of the lower states were frozen, and $3p^6 nln'l'$ configurations were explicitly excluded from the MCHF calculation of the $3p^{-1}$ states of Sc^+.

The resulting thresholds are presented in Table I and compared with available experiment [15] and previous calculations [16]. The agreement of the lowest three threshold with experiment is excellent, indicating that our energy calculations are quite good indeed. The differences of 21, 103, and 38 meV, respectively, for the comparison of the first three theoretical thresholds with experiment. Even for thresholds that are slightly off, however, the various resonance energies are correspondingly off, but the energy of the resonances with respect to their respective thresholds should be considerably more accurate [6].

For the six $3p$ thresholds, no experiment has been reported. However, there are calculated values [16] based on the Cowan code [17], apparently at the single configuration level. Our MCHF results are in general agreement with the older theoretical results, within about 0.4 eV and generally rather better, except for the ^3D threshold which we find to be almost 1 eV larger than the previous result. The ^1D and ^3D levels are degenerate at the HF level, just as the previous result shows. But the introduction of correlations via the MCHF procedure splits them considerably. We believe the present threshold energies to be accurate to a few tenths of an eV, and our level ordering to be correct. In any case, experimental determination of the threshold energies is highly desirable. As with the low-energy resonances, however, even if the threshold energies are somewhat inaccurate, the relative energies of the resonances with respect to their associated thresholds should be considerably more accurate.

C. $3p^5 3d^2 4s^2$ resonance energies

The $3p \rightarrow 3d\ 3p^5 3d^2 4s^2$ resonances are quite strong, and dominate the spectrum over a significant energy region. They are so strong since they are $\Delta n = 0$ transitions and the extent of an orbital is determined largely by the principal quantum number n. This means that initial and final states in the dipole transition occupy the same region of space, thereby allowing significant overlap of the wave functions and, thus, a large dipole matrix element. It is therefore of great importance to get these energies correct, since they affect the cross section, including the other resonances, over an extended energy range. To accomplish this, we have employed the same MCHF methodology used for obtaining good threshold energies. In particular, we employed the same technique that was used for the $3p$ thresholds; even though these $3p^5 3d^2 4s^2\ ^2P,F,D$ odd-parity resonance states are not the lowest of their symmetries, by excluding the HF configurations of the lower states from the MCHF expansion of the resonance states, and fixing the orbitals from the HF calculation of the lowest state of each symmetry, nearly exact orthogonality to the lower states is enforced so that the variational principle produces upper bounds as in the case of the thresholds. In each case, of the order of 500 basis states were used in the MCHF calculation, and the orthogonality among resonances of the same symmetry was enforced so that it is believed that the energies of the higher $3d^2$ resonances of each symmetry are just as accurate as the lowest.

In the matrix diagonalization technique, discussed in Sec. II A, however, energies of resonances are modified by the interaction with other states. To allow this to occur in the case of these resonance states interacting with other discrete states would involve double counting, since the MCHF calculation has already taken these interactions into account. Thus, in that part of the calculation, these $3p^5 3d^2 4s^2$ resonances are treated as separate channels, and the interactions with other discrete states are omitted, where possible, or suppressed artificially by altering the relevant energy denominators to suppress the interaction with other discrete states; the interaction with continuum states is not altered. Aside from an energy shift, interaction with continuum states gives an imaginary part to the energy, which gives the resonances their width.

To be entirely consistent, instead of the MCHF approximation, a configuration interaction employing the MBPT orbitals should have been used to calculate the ''discrete'' part of the resonance energies. To obtain a result of the same quality as the MCHF result would require far more than the approximate 500 basis states used for the MCHF approximation, possibly several orders of magnitude more, which was beyond the capabilities of our codes. In addition, the overlap of our MCHF wave functions with the continuum channel wave functions were quite small, so we had near orthogonality, except near the continuum thresholds. Since these thresholds are far from the resonance energies, this is not very

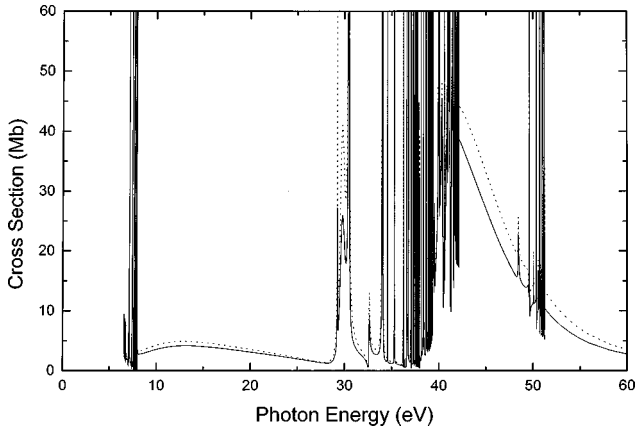

FIG. 1. Calculated total photoionization cross section for the ground state of atomic Sc. The solid line is the length result, and the dotted line is velocity.

important owing to the large energy denominator in such interactions. The use of the MCHF approximation for these resonance energies, then, does in fact involve some double counting since it includes some of the MBPT continuum. But we believe that the methodology employed, while not perfect, is an excellent compromise and leads to accurate results as will be seen below.

III. RESULTS AND DISCUSSION

A. Total cross section

The total photoionization cross section, summed over all channels is shown in Fig. 1. Although the primary focus of this work is the region of $3p$ excitation/ionization, 25–60 eV, the full range from threshold to 60 eV is presented for completeness. The cross section shows three distinct regions. For the first 1 eV or so above the lowest ($3p^6 3d4s\ ^3D$) threshold, the cross section is dominated by Rydberg resonances leading up to the $3p^6 3d4s\ ^1D$ and $3p^6 4s^2\ ^1S$ thresholds. This energy region is shown in greater detail in Fig. 2(a), where three autoionizing series leading up to the ^1D threshold just above 6.6 eV and two series leading up to the ^1S threshold just below 8 eV are clearly seen.

The next region, from the $3p^6 4s^2\ ^1S$ threshold to about 25 eV, is seen to be devoid of resonances; a gradual increase from the ^1S threshold, with a maximum roughly 4 Mb at about 12 eV, followed by a gradual decrease to about 2 Mb at 25 eV. This is due to the $3d \rightarrow \varepsilon f$ delayed maximum of the $3p^6 3d4s^2\ ^2D \rightarrow 3p^6 4s^2 \varepsilon f\ ^2F$ transition, which is basically a single-particle transition since the $3d$ electron represents the only open shell in ground-state Sc.

The photon-energy region from 25 to 60 eV is dominated by resonances leading up the six $3p$ thresholds, seen in Fig. 1, and shown in finer detail in Figs. 2(b)–2(d). But aside from the resonances, there is a strong nonresonant background cross section, as large as about 30 Mb, above 40 eV which falls off with increasing energy. This background cross section is primarily the summation of the various open $3p \rightarrow \varepsilon d$ channels (the $3p \rightarrow \varepsilon s$ channels are small, as are the $4s$ and $3d$ channels here) and is rather similar in magnitude and shape to photoionization of the $3p$ shell in Ar [4,9] and K^+ [18].

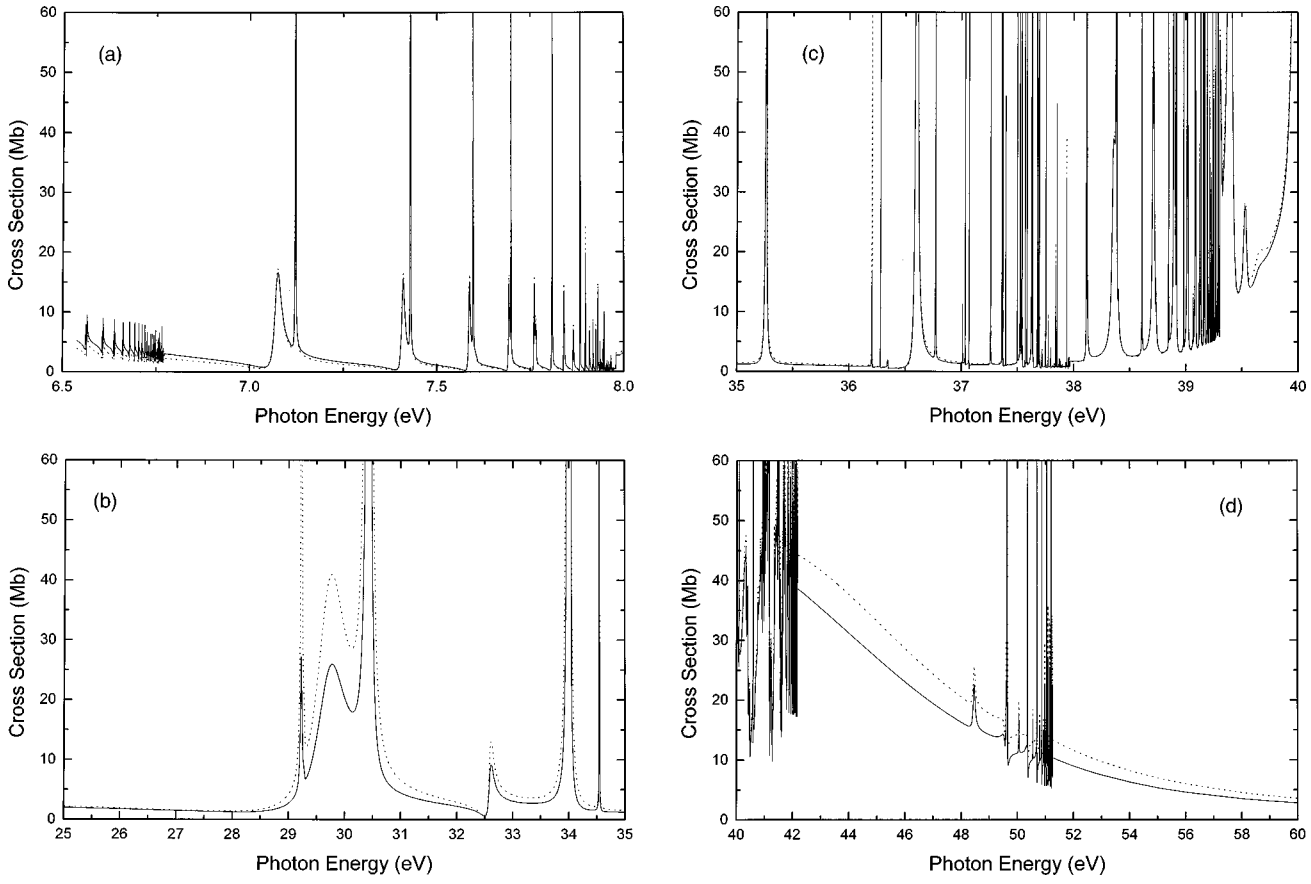

FIG. 2. Calculated total photoionization cross section for the ground state of atomic Sc, and details of each energy region: (a) 6.5–8.0 eV, (b) 25–35 eV, (c) 35–40 eV, and (d) 40–60 eV. The solid line is the length result, and the dotted line is velocity.

Note that both Figs. 1 and 2 present length and velocity results, and the agreement between them is quite good, generally within 15% or better. Although this agreement is not a conclusive test, it is believed to be indicative of the accuracy of the calculated cross sections. In particular, this agreement suggests that the omission of ionization plus excitation channels in this calculation, notably for transitions to $3p^6 3d^2$ and $3p^5 3d^2 4s$ final states of Sc^+, does not significantly affect the cross sections (background or resonant) of the channels included.

There are some experimental data on the photoionization of atomic Sc in the 30–50-eV photon-energy region [5]. These are, however, only relative data, so we can compare only incompletely. Nevertheless, if we add an instrumental function to broaden our resonances to approximately the experimental resolution, the shapes are generally the same. The dominant feature of the experimental curve (Fig. 27 of Ref. [5]) is a broad maximum centered at about 40 eV surmounted with significant resonances, particularly on the low-energy side, along with resonances in the 30-eV region surmounted on a smallish background. This is what is found in the calculated results as well.

B. $3p \rightarrow 3d$ resonances

The strongest resonances seen in Figs. 1 and 2 are the nine $3p \rightarrow 3d$ resonances, $[\mathrm{Mg}]3p^5 3d^2 4s^2$. They dominate the cross section in the 25–35-eV region, shown in Fig. 2(b), which include six of these resonances, several of which are extraordinarily wide and strong. The complex of three resonances in the 29–31-eV region alone contain a total oscillator strength of the order of unity. Note that there are actually three sets of two resonances corresponding to ^2P, ^2D, and ^2F final states, and these different symmetry resonances have rather different characteristics.

The detailed identification of each resonance is given in Table II. The cross sections for the individual *LS* channels are presented in Fig. 3. From Fig. 3(a), it is evident that the ^2P resonances are quite narrow and rather symmetric. The symmetry is due to the fact that the underlying continuum cross sections, $4s \rightarrow \varepsilon p$ and $3d \rightarrow \varepsilon p$, are quite small this far above their thresholds. The ^2D resonances, [Fig. 3(b)] are much stronger and wider, and also quite symmetric. Again, this symmetry is owing to the fact that the underlying continua can only be produced by $4s \rightarrow \varepsilon p$ transitions which are, as in the ^2P case, rather weak so far above threshold. If this symmetry explanation is correct, then the ^2F resonances, which are surmounted on a strong $3d \rightarrow \varepsilon f$ cross section, should be rather asymmetric. Looking at the ^2F resonances in Fig. 3(c), that is exactly what is seen. Furthermore, the ^2F resonances are quite broad, the lowest being ~ 1 eV in width. And the lowest is the strongest (largest oscillator strength) of all of the $3p \rightarrow 3d$ resonances.

The three higher-energy $3p \rightarrow 3d$ resonances, ^2P, ^2D, and ^2F, are mixed among the various $3p \rightarrow ns$ and $3p \rightarrow nd$ Rydberg resonances leading up to the six $3p^5 3d 4s^2$ thresholds of Sc^+. Owing to the close proximity to a number of other resonances of different configurations with the same *LS* symmetry, each of these higher-energy $3p \rightarrow 3d$ resonances is strongly mixed through interchannel coupling, and its oscillator strength distributed over a number of resonances. They are, therefore, much weaker than their lower-energy counterparts, as well as being somewhat narrow. They are, however, identifiable and they are also presented in Table II. These higher-energy $3p \rightarrow 3d$ resonances will thus be discussed in a subsequent paper, along with the Rydberg resonances with which they are so significantly intermixed.

TABLE II. Energies of the $3p^5 3d^2 4s^2$ resonances in eV. The designation of each resonance is given as the coupling of $3d^2$ in parentheses, and the total coupling, e.g., $\{3p^5(3d^2\ ^1D)4s^2\}^2P$ is the full primary designation of the first entry. The resonances are not pure and the admixture among the various possible $3d^2$ couplings resulting from the MCHF calculation are also given; note that these are the absolute values of coefficients, not probabilities. Note also that the mixings resulting from interchannel coupling, crucial for the determination of the resonance energy, are not given in this table; the energies given do include these mixings. The experimental energies are from Ref. [5].

Primary designation	Admixture			Energy	Experiment
$(^1D)^2P$	$0.78(^1D)$	$0.34(^1S)$	$0.44(^3P)$	29.23	
$(^1S)^2P$	$0.43(^1D)$	$0.85(^1S)$	$0.07(^3P)$	34.55	
$(^3P)^2P$	$0.33(^1D)$	$0.23(^1S)$	$0.78(^3P)$	40.00	
$(^1D)^2D$	$0.85(^1D)$	$0.10(^3P)$	$0.44(^3F)$	30.43	30.7, 31.1
$(^3P)^2D$	$0.22(^1D)$	$0.90(^3P)$	$0.24(^3F)$	33.99	
$(^3F)^2D$	$0.39(^1D)$	$0.31(^3P)$	$0.82(^3F)$	39.54	
$(^1G)^2F$	$0.70(^1G)$	$0.18(^1D)$	$0.67(^3F)$	29.68	29.6, 29.7
$(^1D)^2F$	$0.09(^1G)$	$0.94(^1D)$	$0.11(^3F)$	32.59	
$(^3F)^2F$	$0.65(^1G)$	$0.04(^1D)$	$0.68(^3F)$	39.95	

The great strength of the $3p \rightarrow 3d$ resonances is principally due to the fact that these are $\Delta n = 0$ transitions. Furthermore, since Sc is a transition metal, the $3d$ orbital is ''collapsed,'' i.e., it is bound in the inner well of the double-welled effective *d*-wave potential [19]. Then, since the ''size'' of an orbital is determined by the principal quantum number *n*, and very little else, it is clear the $3p$ and $3d$ orbitals occupy the same region of space, leading to a very large overlap. This translates into a very large dipole matrix element which, of course, means a large oscillator strength. Thus, despite the fact that the coupling with the $3d$ electron in the ground state breaks this $3p \rightarrow 3d$ oscillator strength into nine distinct transitions, the six $3p \rightarrow 3d$ resonances in the 25–35-eV range *all* have very significant strength, as seen in Fig. 2.

The Auger electron energies generated by these six strong resonances can easily be obtained from the resonance energies (Table II) and the threshold energies (Table I). The strengths of their decay to the various possible decay channels are given in Fig. 4. Note that the autoionizing transitions to both $3p^6 3d 4s\ ^3D$ and ^1D Sc^+ states are $3d4s \rightarrow 3p\varepsilon p$ transitions, while autoionization to the $3p^6 4s^2\ ^1S$ Sc^+ can be either $3d^2 \rightarrow 3p\varepsilon p$ or $3d^2 \rightarrow 3p\varepsilon f$. Looking at the lowest ^2P resonance, note from Table II that $3d^2$ is coupled mostly to ^1D with some ^1S as well. Thus, from the point of view of angular momentum geometry, the coupling with the ^3D final state is quite weak, as is the coupling with the ^1S final state, while the coupling with the ^1D of Sc^+ is far stronger; thus virtually all of the strength goes into the ^1D state, as seen in Fig. 4, with just a little going into the ^1S state. It is also the

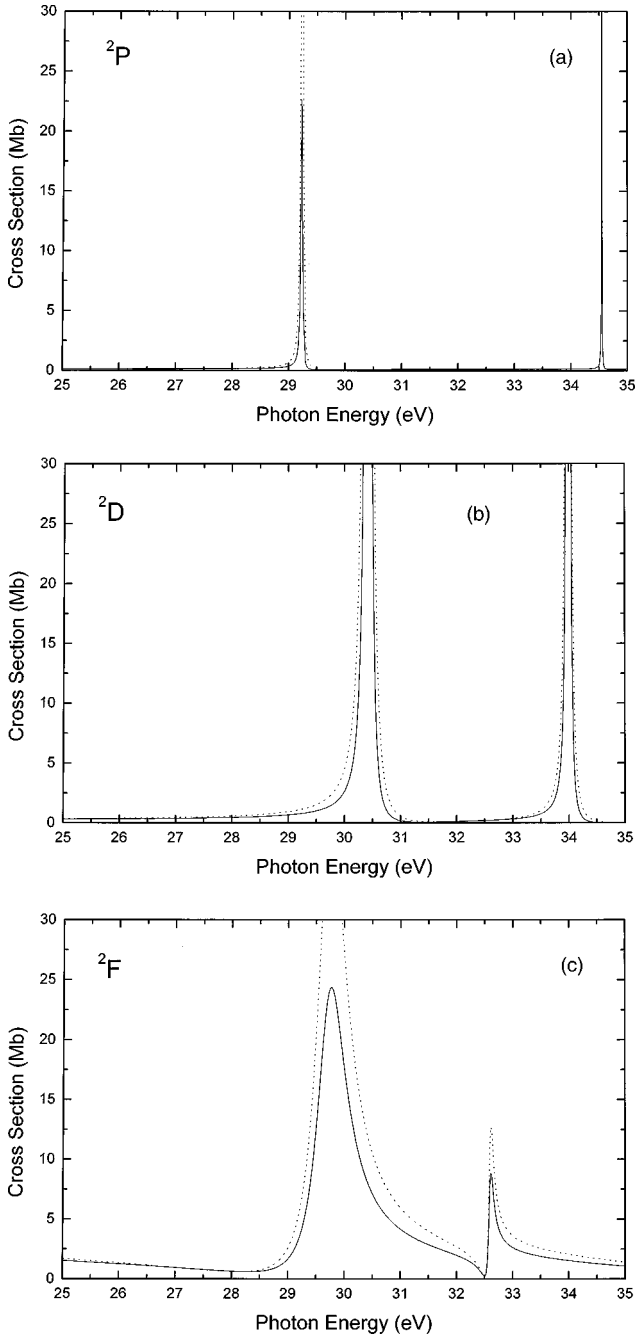

FIG. 3. Calculated total *LS* cross sections for photoionization of atomic Sc in the 25–35-eV photon energy range: (a) ^2P total, (b) ^2D total, and (c) ^2F total. The solid line is the length result, and the dotted line is velocity.

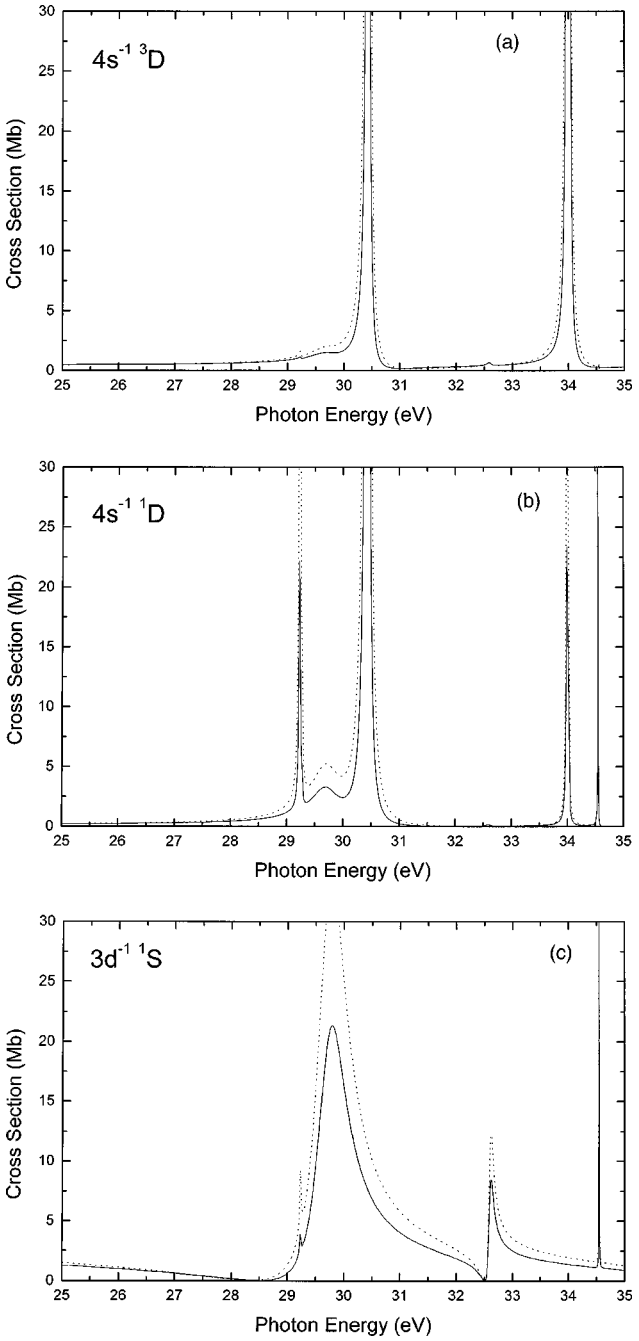

FIG. 4. Calculated photoionization cross sections for atomic Sc leading to the (a) $4s^{-1}\,^3D$, (b) $4s^{-1}\,^1D$, and (c) $3d^{-1}\,^1S$ states of Sc^+. The solid line is the length result, and the dotted line is velocity.

case that the radial autoionization (Coulomb) matrix element for a $3d4s \rightarrow 3p\varepsilon p$ transition is significantly larger, in this energy range, than for a $3d^2 \rightarrow 3p\varepsilon p$ transition; the $4s$ orbital overlaps with εp better than the $3d$ orbital, predominantly since the $4s$ orbital has a greater radial extent. Thus, the radial part of the matrix element mitigates against decay to the Sc^+ ^1S channel, so it is reduced, even though there is some ^1S in the resonance.

The higher ^2P resonance, which is coupled primarily to ^1S with some ^1D, is explained similarly. There is, as in the previous case, virtually no possibility of decaying to the ^3D Sc^+ channel. The increase of the coupling of $3d^2$ to ^1S, with respect to ^1D, means that the strength of this resonance in the ^1S final channel will increase relative to the ^1D, as compared to the previous case; this is exactly what is seen in Fig. 4(a). The fact that the ^1D channel is still the dominant decay final state speaks to the importance of the radial wave functions and overlaps. From this explanation it is clear that angular momentum geometry alone cannot explain the decay patterns; dynamical (radial wave function) information is also required.

The ^2D resonances present a simpler case because transitions to the Sc^+ ^1S channel are forbidden. The $3d \rightarrow \varepsilon p$, εf transitions can only lead to ^2P or ^2F, not ^2D. Then, going

through a similar analysis as for the ^2P resonances, we find the lowest ^2D resonance, primarily ^1D with a strong ^3P admixture, decays most strongly to the ^1D final state and, since there is a significant triplet admixture, has a very significant ^3D cross section as well. For the higher ^2D resonance, the triplet portion of the $3d^2$ is somewhat larger than the ^1D, and in this case the cross section for the final ^3D state dominates.

Finally, for the ^2F resonances, angular momentum considerations become less important, and radial matrix elements dominate. In particular, $3d^2 \rightarrow 3p\varepsilon f$, which can only occur in a ^2F channel, is very significantly larger than any other radial matrix element for the decay process. Thus the cross section to the $^1S\varepsilon f\ ^2F$ final state should dominate, and indeed it does, as seen in Fig. 4(c). Small probabilities of the lower of the ^2F resonances are seen in the ^3D and ^1D channels, and these can be explained via angular momentum geometry considerations as above.

Note that no mention has been made of another possible decay mode, decay to $3p^6 3d^2$ Sc^+ channels. These channels represent ionization plus excitation, and are not included in the calculation since they are likely to be quite small. Furthermore, the decay of $3p^5 3d^2 4s^2$ resonances to any of these channels is also likely to be quite insignificant compared to the other decay channels discussed above. This is because the decay to $3p^6 3d^2 \varepsilon p$ final states requires a $4s^2 \rightarrow 3p\varepsilon p$ autoionizing transition. Then since $4s$ and $3p$ orbitals occupy rather different regions of space, the $4s$ being of much larger spatial extent, their overlap is small; thus the autoionization matrix element, which is the matrix element of $1/r_{12}$ (which emphasizes the inner region), is quite small. Thus this autoionizing transition matrix element is very much smaller than $3d4s \rightarrow 3p\varepsilon p$ or $3d^2 \rightarrow 3p\varepsilon d$, since a $3d$ orbital is involved in each transition; $3p$ and $3d$ orbitals occupy the same region of space, and the overlap is large. For these reasons, it is estimated that the omitted decay channels have cross sections for the $3p \rightarrow 3d$ resonances of 1–2 orders of magnitude smaller that the channels included, where a $3d$ orbital is involved in the decay. This is the justification for the omission of $3p^6 3d^2$ final states of Sc^+ in the calculation.

Some of the positions of the resonances have been reported experimentally [5], and tentatively identified with the aid of relatively simple calculations. The resonances occur in pairs owing to the small spin-orbit splitting, but the centroid should represent a reasonable nonrelativistic result, especially since the reported error bars (± 0.1 eV) are of the same size as the splitting. Five resonances are given; however, three of them are in the region where Rydberg resonances abound, and we do not believe that they are $3p^5 3d^2 4s^2$ resonances. Of the other two, the lowest pair is at 29.6 and 29.7 eV (Table II), in excellent agreement with our calculated lowest ^2F resonance, and we agree with their tentative assignment. The pair at 30.7 and 31.1 eV are slightly above our prediction for the lowest ^2D resonance, which we believe to be the correct assignment for the pair, especially in view of the calculated strength of the lowest ^2D resonance; it seems much more likely that the experiment detected this resonance than the very much smaller second ^2F resonance which is the previous tentative assignment [5].

The other three resonances are probably Rydberg resonances. The pair at 35.2 and 35.3 eV, for example, are clearly the very strong $\{3p^5 3d4s^2\ ^3P\ 5s\}^2P$ resonance which we find at 35.26 eV, seen clearly in Fig. 2. The pair at 36.7 and 36.9 eV matches reasonably well with the strong $\{3p^5 3d4s^2\ ^3F\ 5s\}^2F$ resonance at 36.60 eV, also seen in Fig. 2. And the pair at 37.9 and 38.2 eV could be the strong $\{3p^5 3d4s^2\ ^1D\ 5s\}^2F$ resonance found at 38.38 eV. This will be discussed more fully in a subsequent paper, where the details of the Rydberg resonances will be discussed in detail.

IV. CONCLUDING REMARKS

A theoretical methodology for the calculation of photoionization of open-shell atoms has been presented which combines MBPT for weak perturbations, a coupled-channel formalism augmented by perturbation theory for the strong interchannel interactions, and the MCHF approximation to produce accurate energies. This completely *ab initio* theory has the distinct advantage of being able to include or omit various aspects of correlation based upon the physics of the particular problem. Or, looked at in an alternate manner, it allows us to determine which are the important aspects of correlation completely theoretically by investigating the magnitude of the effect(s) of including or omitting a particular term.

The method has been applied to the photoionization cross section of atom Sc, the first of the transition-metal atoms. Over a broad energy range, the cross section was found to be dominated by $3p \rightarrow 3d$ autoionizing resonances. Agreement of the total cross section and the resonance positions with available experiment was quite good. It would, however, be quite useful for more extensive and detailed measurements to be carried out to fully assess theory. In a subsequent paper, the detailed theoretical partial cross sections for each channel, along with the detailed positions and assignments of the Rydberg resonances, will be presented.

This work represents the initial phase of a larger project of theoretical study of the photoionization of ground and excited states of atoms and ions with open *nd* subshells, particularly the transition-metal atoms. Depending upon their importance for any particular case, ionization plus excitation channels can be included in a straightforward manner. Inclusion of spin-orbit splittings and shifts provide a bit of a challenge. For the energies, this can be handled perturbatively within the existing MCHF framework [14]. For the dipole matrix elements, this will be effected by assuming that radial wave functions are not affected by spin-orbit interactions and recoupling the various discrete and continuum states from *LS* to *jj*. This addition is currently in progress.

ACKNOWLEDGMENTS

This work was supported by the NSF and NASA. Numerous discussions with C. F. Fischer through the initial phase of this work are gratefully acknowledged.

[1] *Applied Atomic Collision Physics*, edited by H. S. W. Massey, E. W. McDaniel, and B. Bederson (Academic, New York, 1983), Vols. 1–5.

[2] S. T. Manson, in *Photoemission in Solids I*, edited by M. Cardona and L. Ley (Springer-Verlag, Berlin, 1978), pp. 135–163.

[3] *New Directions in Research With Third-Generation Soft X-Ray Synchrotron Radiation Sources*, Vol. 254 of *NATO Advanced Study Institute Series E: Applied Sciences*, edited by A. S. Schlachter and F. J. Wuilleumier (Kluwer, Dordrecht, 1992).

[4] V. Schmidt, Rep. Prog. Phys. **55**, 1483 (1992), and references therein.

[5] B. Sonntag and P. Zimmermann, Rep. Prog. Phys. **55**, 911 (1992), and references therein.

[6] F. Robicheaux and C. H. Greene, Phys. Rev. A **48**, 4429 (1993).

[7] F. Robicheaux and C. H. Greene, Phys. Rev. A **48**, 4441 (1993).

[8] J. J. Boyle, Z. Altun, and H. P. Kelly, Phys. Rev. A **47**, 4811 (1993).

[9] A. F. Starace, in *Handbuch der Physik*, edited by W. Mehlhorn (Springer-Verlag, Berlin, 1982), Vol. 31, pp. 1–121.

[10] H. A. Bethe and E. E. Salpeter, *Quantum Mechanics of One- and Two-Electron Atoms* (Springer-Verlag, Berlin, 1957), pp. 248–252.

[11] C. Froese Fischer, *The Hartree-Fock Method For Atoms* (Wiley-Interscience, New York, 1977).

[12] J. J. Boyle, Phys. Rev. A **48**, 2860 (1993).

[13] H. P. Kelly, Adv. Theor. Phys. **2**, 75 (1968).

[14] C. Froese Fischer, Comput. Phys. Commun. **64**, 369 (1991).

[15] *Atomic Energy Levels*, edited by C. E. Moore, Natl. Bur. Stand. (U.S.) Circular No. 467 (U.S. GPO, Washington, DC, 1949).

[16] M. Meyer, Th. Prescher, E. von Raven, M. Richter, E. Schmidt, B. Sonntag, and H.-E. Wetzel, Z. Phys. D **2**, 347 (1986).

[17] R. D. Cowan, *The Theory of Atomic Structure and Spectra* (University of California Press, Berkeley, 1981).

[18] G. Nasreen, P. C. Deshmukh, and S. T. Manson, J. Phys. B **21**, L281 (1988).

[19] A. R. P. Rau and U. Fano, Phys. Rev. **167**, 7 (1968).